Folding of *Escherichia coli* DsbC: Characterization of a Monomeric Folding Intermediate†

Huimin Ke,‡,§ Sen Zhang,‡,§ Jian Li,‡,§ Geoffrey J. Howlett,|| and Chih-chen Wang*,‡

National Laboratory of Biomacromolecules, Institute of Biophysics, Chinese Academy of Sciences, 15 Datun Road, Beijing 100101, China, Graduate School of the Chinese Academy of Sciences, Beijing 100049, China, and Department of Biochemistry and Molecular Biology and Bio21 Molecular Science and Biotechnology Institute, University of Melbourne, Parkville, Victoria 3010, Australia

Received July 27, 2006; Revised Manuscript Received October 4, 2006

ABSTRACT: The homodimeric protein DsbC is a disulfide isomerase and a chaperone located in the periplasm of *Escherichia coli*. We have studied the guanidine hydrochloride (GdnHCl)-induced unfolding and refolding of DsbC using mutagenesis, intrinsic fluorescence, circular dichroism spectra, size-exclusion chromatography, and sedimentation velocity analysis. The equilibrium refolding and unfolding of DsbC was thermodynamically reversible. The equilibrium folding profile measured by fluorescence excited at 280 nm exhibited a three-state transition profile with a stable folding intermediate formed at 0−2.0 M GdnHCl followed by a second transition at higher GdnHCl concentrations. Sedimentation velocity data revealed dissociation of the dimer to the monomer over the concentration range of the first transition (0−2.0 M). In contrast, fluorescence emission data for DsbC excited at 295 nm showed a single two-state transition. Fluorescence emission data for the equilibrium unfolding of the monomeric G49R mutant, excited at either 295 or 280 nm, indicated a single two-state transition. Data obtained for the dimeric Y52W mutant indicated a strong protein concentration dependence of the first transition but no dependence of the second transition in equilibrium unfolding. This suggests that the fluorescence of Y52W sensitively reports conformational changes caused by dissociation of the dimer. Thus, the folding of DsbC follows a three-state transition model with a monomeric folding intermediate formed in 0−2.0 M GdnHCl. The folding of DsbC in the presence of DTT indicates an important role for the non-active site disulfide bond in stabilizing the conformation of the molecule. Dimerization ensures the performance of chaperone and isomerase functions of DsbC.

Disulfide bonds are important for the folding, stability, and function of many proteins. The Dsb family proteins in the periplasm of prokaryotic cells comprise at least six members (DsbA, DsbB, DsbC, DsbD, DsbE, and DsbG) and are thiol-disulfide oxidoreductases responsible for the formation of native disulfide bonds in newly synthesized proteins (*1*). DsbC is a soluble homodimeric protein that catalyzes the rearrangement of disulfide bonds and is therefore considered a prokaryotic counterpart of the eukaryotic protein disulfide isomerase that is located in the endoplasmic reticulum (*2*). Like protein disulfide isomerase, DsbC also has intrinsic chaperone activity (*3*). The N-terminal sequence of DsbC (residues 1−65) is essential not only for dimer formation but also for isomerase and chaperone activities (*4*). Crystal structure analysis reveals that DsbC is a V-shaped homodimer with each subunit forming an arm of the V (*5*). The C-terminal thioredoxin-like domain is linked via a hinged linker helix to the N-terminal domain, which is responsible for dimerization (Figure 1). The active sites, Cys^{98}-Gly-Tyr-Cys^{101}, in both thioredoxin-like domains of DsbC are essential for isomerase activity, while only one is required for oxidoreductase activity (*4*). Substitution of Gly^{49} with Arg converts the dimeric disulfide isomerase into a monomeric oxidase (*6*). Linkage of monomeric Trx,[1] DsbA, or the *a* domain of protein disulfide isomerase, each of which individually has no or low isomerase and chaperone activity, to the association domain of DsbC forms a dimeric molecule, which is endowed with both isomerase and chaperone activities (*7*).

In addition to a disulfide bond in the active site of each subunit, there is a non-active site disulfide bond, Cys^{141}−Cys^{163}, which was suggested to play a purely structural role (*2*). Via specific replacements of Cys with Ser, we have shown that the active site disulfide bond is necessary for enzyme but not for chaperone activity; in contrast, the non-active site disulfide bond is not required for enzyme activity but plays an important role in folding, stability, export, and the chaperone activity of the molecule (*8*). GdnHCl-induced unfolding of DsbC monitored using intrinsic fluorescence excited at 297 nm indicates a reversible two-state process (*9*).

† This work was supported by the National Natural Science Foundation of China (30470363), the Chinese Ministry of Science and Technology (2006CB806508), and the Chinese Academy of Sciences.

* To whom correspondence should be addressed: National Laboratory of Biomacromolecules, Institute of Biophysics, Chinese Academy of Sciences, 15 Datun Rd., Beijing 100101, China. Telephone: +86-10-64888502. Fax: +86-10-64872026. E-mail: chihwang@sun5.ibp.ac.cn.

‡ National Laboratory of Biomacromolecules, Institute of Biophysics, Chinese Academy of Sciences.

§ Graduate School of the Chinese Academy of Sciences.

|| University of Melbourne.

[1] Abbreviations: GdnHCl, guanidine hydrochloride; ANS, 8-anilino-1-naphthalenesulfonic acid; DTT, dithiothreitol; CD, circular dichroism; Trx, thioredoxin.

10.1021/bi061511m CCC: $33.50
Published on Web 11/18/2006

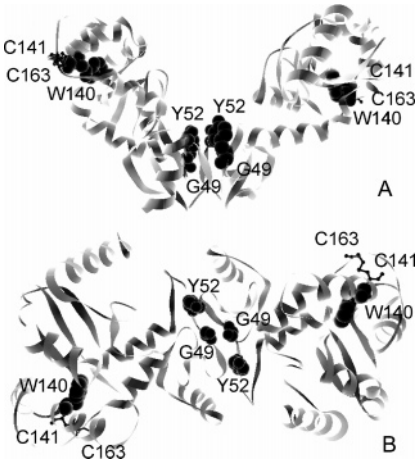

FIGURE 1: Ribbon representations of the crystal structure of DsbC from the front (A) and top (B). The localizations of Gly^{49}, Tyr^{52}, and Trp^{140} are shown as solid van der Waals spheres; Cys^{141} and Cys^{163} are represented by sticks and balls. This figure was prepared using PDB entry 1EEJ (*5*) and 3D Molecular Viewer, a component of Vector NTI Suite 9.0.0.

In this study, we have monitored the unfolding process by intrinsic fluorescence with excitation at either 295 or 280 nm. By comparison of the thermodynamic and kinetic unfolding data for wild-type dimeric DsbC and two single-site mutants, dimeric Y52W and monomeric G49R, we show that the unfolding of dimeric DsbC occurs via a stable monomeric folding intermediate formed in an initial transition at low GdnHCl concentrations. Our results provide further evidence of the important role of dimerization in the function of DsbC as both an isomerase and a chaperone, and the role of the unique non-active site disulfide bond in stabilizing the structure of DsbC.

MATERIALS AND METHODS

Materials. 8-Anilino-1-naphthalenesulfonic acid (ANS) and cCMP were purchased from Sigma. GdnHCl was from Gibco and 5,5′-dithiobis(2-nitrobenzoic acid) from Fluka. Dithiothreitol (DTT) and isopropyl 1-thio-β-D-galactoside were from Serva. All other chemicals were local products of analytical grade. In all experiments, 0.1 M potassium phosphate buffer containing 2.5 mM EDTA (pH 7.5) was used and termed phosphate buffer.

Preparations. Plasmid pDsbC containing the full-length DsbC precursor gene was a generous gift from R. Glockshuber (Eidgenössische Technische Hochschule Hönggerberg, Zurich, Switzerland). Plasmids of pG49R and pY52W were constructed by PCR using pDsbC as a template. The DsbC proteins were purified using the method of Liu et al. (*8*). The concentration of the DsbC protomer was determined spectrophotometrically at 280 nm with an ϵ_{280} of 16 170 M^{-1} cm^{-1} (*2*). The concentration of G49R and Y52W was determined by the Bradford method (*10*) with DsbC as a standard. D-Glyceraldehyde-3-phosphate dehydrogenase was prepared from rabbit muscle (*11*). Thiol group was determined using 5,5′-dithiobis(2-nitrobenzoic acid) (*12*).

Equilibrium Experiments. DsbC and its mutant derivatives at a range of concentrations (DsbC at 1, 5, and 20 μM, Y52W at 0.5, 1, 2, 5, and 20 μM, and G49R at 5 μM) were unfolded via incubation with GdnHCl at various concentrations in the presence and absence of 0.1 M DTT at 25 °C for 20 h to reach equilibrium. Intrinsic fluorescence spectra with excitation at 280 and 295 nm were measured on a Shimadzu RF-5301PC or a Hitachi F-4500 spectrofluorometer, and circular dichroism (CD) spectra were recorded from 200 to 250 nm on a Jasco 500 spectropolarimeter at 25 °C.

Refolding of 250 μM proteins fully denatured in 4 M GdnHCl for 20 h at 25 °C in the presence and absence of 0.1 M DTT was triggered by 50-fold dilution into a phosphate buffer containing GdnHCl at different concentrations (as well as 0.1 M DTT in the case of denatured and reduced DsbC), and the sample was then incubated at 25 °C for 2 h before fluorescence measurement.

The phase diagram analysis was built up of I_{320} versus I_{365} (fluorescence intensity at 320 and 365 nm, respectively) excited at 295 nm and of I_{315} versus I_{345} excited at 280 nm under different unfolding conditions for a protein undergoing structural transformations (*13*).

Size-Exclusion Chromatography. Protein (50 μL) was loaded on either a SEC 250-5 (Bio-Rad) or a Superdex 75 HR 10/30 column (Pharmacia) pre-equilibrated with the same concentration of GdnHCl as in the sample (including 5 mM DTT if the unfolding was performed in the presence of DTT) and eluted at 1 mL/min in SEC 250-5 or 0.5 mL/min in Superdex 75 HR 10/30.

Sedimentation Velocity Experiment. Samples were analyzed using an XL-A analytical ultracentrifuge (Beckman Coulter, Fullerton, CA) equipped with an AnTi60 rotor at 20 °C. Samples and control reference buffer (approximately 360 μL) were added to double-sector epon-filled centerpieces and radial absorbance data at 280 nm acquired at 5 min intervals, radial increments of 0.002 cm in continuous scanning mode, and a rotor speed of 40 000 rpm. The sedimentation velocity data were fitted to obtain a molecular mass distribution, $c(M)$, assuming a distribution of diffusible species with a range of molecular weights from 1000 to 100 000 (*14*) and using assigned values for the density and viscosity of the buffers and GdnHCl solutions (*15*). The frictional coefficient was varied during the fitting procedure to obtain the best-fit value. Good fits to the data were obtained as indicated by the random distribution of residuals, allowing the molecular mass distributions to be integrated to obtain the weight-average molecular weights for the samples (*14*).

Kinetics Experiments. Kinetics of refolding and unfolding of proteins was monitored by fluorescence spectroscopy using an Applied Photophysics model PiStar180 stopped-flow spectrophotometer for the fast phase and a Hitachi model device F-4500 for the slow phase. Emission was monitored at 315 and 320 nm for excitation at 280 and 295 nm, respectively. For unfolding experiments, proteins were diluted 11-fold in a buffer containing 3.3 M GdnHCl; for refolding experiments, proteins fully denatured in 3.0 M GdnHCl at 25 °C overnight were diluted 11-fold in phosphate buffer. The final concentration of proteins was 5 μM.

Activity Assay. Thiol-disulfide reductase activity was assayed by measuring the turbidity increase at 650 nm due to insulin reduction. DTT (1 mM) was added to 0.1 M potassium phosphate (pH 6.6) containing 0.13 mM bovine insulin in the absence and presence of DsbC proteins (*16*). Activity was expressed as a ratio of the slope of a linear part in the turbidity curve to the lag time (*17*). Isomerase activity was assayed according to the reactivation of scrambled

Table 1: Equations for the Equilibrium Unfolding of DsbC Proteins[a]

two-state model	three-state model via a monomeric intermediate	eq
equilibrium		
$N \overset{K_{NU}}{\longleftrightarrow} U$	$N_2 \overset{K_{NI}}{\longleftrightarrow} 2I \overset{K_{IU}}{\longleftrightarrow} 2U$	1
law of mass action		
$K_{NU} = [U]/[N]$	$K_{NI} = [I]^2/[N_2]$	2
	$K_{IU} = [U]/[I]$	3
additivity of the signals		
$y = f_N(y_N + m_N[\text{GdnHCl}]) + f_U(y_U + m_U[\text{GdnHCl}])$	$y = f_N(y_N + m_N[\text{GdnHCl}]) + f_I y_I + f_U(y_U + m_U[\text{GdnHCl}])$	4
variations of ΔG with [GdnHCl]		
$\Delta G_{NU} = -RT \ln K_{NU} = \Delta G_{NU}^{H_2O} - m_{NU}[\text{GdnHCl}]$	$\Delta G_{IU} = -RT \ln K_{IU} = \Delta G_{IU}^{H_2O} - m_{IU}[\text{GdnHCl}]$	5
	$\Delta G_{NI} = -RT \ln K_{NI} = \Delta G_{NI}^{H_2O} - m_{NI}[\text{GdnHCl}]$	6
definition of the molar fractions		
$f_N = [N]/P$; $f_U = [U]/P = f_N K_{NU}$	$f_I = [I]/P$; $f_N = 2[N_2]/P = \dfrac{2Pf_I^2}{K_{NI}}$; $f_U = [U]/P = f_I K_{IU}$	7−9
solving equations		
$1 = f_N + f_U = f_N(1 + K_{NU})$	$1 = f_N + f_I + f_U = \dfrac{2Pf_I^2}{K_{NI}} + f_I + f_I K_{IU}$	10
	$2Pf_I^2 + [K_{NI}(1 + K_{IU})]f_I - K_{NI} = 0$	11
$f_N = \dfrac{1}{1 + K_{NU}}$	$f_I = \dfrac{-K_{NI}(1 + K_{IU}) + \sqrt{[K_{NI}(1 + K_{IU})]^2 + 8PK_{NI}}}{4P}$	12
	$\Delta G_{NU}^{H_2O} = \Delta G_{NI}^{H_2O} + \Delta G_{UI}^{H_2O}$	13
	$m = m_{NI} + m_{IU}$	14

[a] Abbreviations: N_2/N, native dimeric/monomeric state; I, monomeric intermediate state; U, unfolded state; y, measured global fluorescence intensity; y_N and y_U, intercepts of the initial and final baselines, respectively; m_N and m_U, slopes of the initial and final baselines, respectively; y_I, fluorescence intensity for the intermediate state, which is assumed not to vary with GdnHCl concentration to minimize the number of parameters in the fit (*28*); P, total concentration of protein protomers (molar); f_N, f_I, and f_U, fractions of N_2/N, I, and U, respectively; T, temperature (kelvin); R, gas constant; ΔG_{NU}, ΔG_{NI}, and ΔG_{IU}, free energies for unfolding transitions; $\Delta G_{NU}^{H_2O}$, $\Delta G_{NI}^{H_2O}$, and $\Delta G_{IU}^{H_2O}$, free energies for unfolding transitions in the absence of GdnHCl; m_{NU}, m_{NI}, and m_{IU}, slopes of the transitions; NU, NI, and IU, transitions from the native monomeric state to the unfolded state, from the native dimeric state to the monomeric intermediate state, and from the monomeric intermediate state to the unfolded state, respectively. Other parameters are defined in the table. The final fitting equation was obtained by replacing f_N, f_I, and f_U in eq 4 with their expressions as a function of GdnHCl concentration. Equations 4−6 have already been discussed (*29*, *30*).

Table 2: Characterization of DsbC Proteins

protein	molecular mass (kDa): calculated	molecular mass (kDa): size-exclusion chromatography[a]	association state	thiol-disulfide reductase activity[b] ($\times 10^{-3}$ ΔA_{650}/min^{-2})	isomerase activity[b] ($\times 10^{-3}$ μM RNase min^{-1} μM protein^{-1})	chaperone activity
DsbC	23.458	53	dimer	7.7 ± 1.1	61 ± 6	yes
G49R	23.557	35	monomer	0.8 ± 0.4	5.3 ± 2.6	none
Y52W	23.481	54	dimer	7.0 ± 0.5	68 ± 10	yes

[a] In a Superdex 75 HR 10/30 column. [b] Data for protomer are expressed as means ± the standard deviation ($n = 3$).

RNase A (*18*) by monitoring the absorbance increase at 296 nm that resulted from the hydrolysis of cCMP (*19*). Chaperone activity was determined by assessing the reactivation of GdnHCl-denatured D-glyceraldehyde-3-phosphate dehydrogenase upon dilution in the presence of DsbC proteins at different concentrations (*3*).

Data Analysis. Equilibrium folding curves monitored by fluorescence intensity were analyzed using thermodynamic models (*20*) described in eqs 1−14 in Table 1 depending on the observed transition number and the association state of the folding intermediate determined by sedimentation velocity. The folding profiles were fitted to eq 4 with the regression wizard of SigmaPlot, followed by the nonlinear least-squares algorithm.

Kinetic folding curves were fitted to eq 15:

$$F(t) = F(\infty) + \sum_{i=1}^{n} A_i \exp(-k_i t) + Bt \qquad (15)$$

where $F(t)$ and $F(\infty)$ represent the intrinsic fluorescence intensity at time t and infinite time, respectively, A_i is the amplitude corresponding to the individual phase at time zero, k_i is the rate constant of the reaction, and B is the slope of fluorescence attenuation.

RESULTS

Characterization of G49R and Y52W. Figure 1 shows ribbon representations of the crystal structure of DsbC. DsbC, G49R, and Y52W elute on a Superdex 75 HR 10/30 column as a single peak at a position corresponding to apparent molecular mass values of 53, 35, and 54 kDa, respectively (Table 2). The single mutation of Gly^{49} to Arg disrupts the association of DsbC subunits so that the molecule is monomeric, while the mutation of Tyr^{52} to Trp does not. The CD spectra of Y52W and G49R were almost identical to that of DsbC in both the shape and ellipticities at 208 and 222 nm (data not shown).

After treatment with excess DTT under nondenaturing conditions, the DsbC dimer exhibited eight free thiol groups, indicating that both disulfide bonds, Cys^{98}−Cys^{101} and

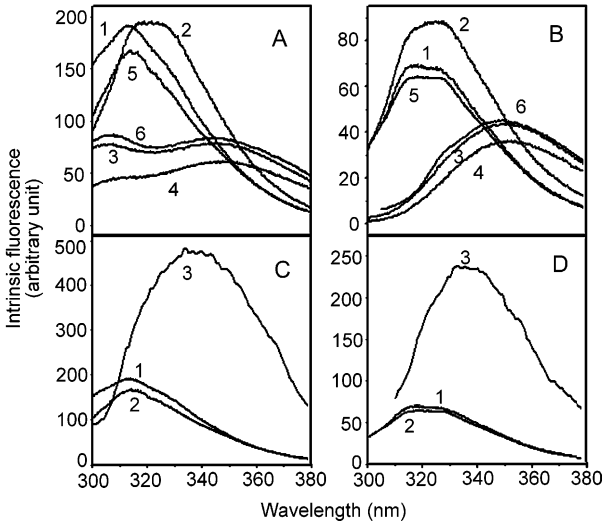

FIGURE 2: Intrinsic fluorescence spectra of DsbC proteins. Fluorescence spectra of DsbC proteins at 5 μM were measured with excitation at 280 (A and C) and 295 nm (B and D). (A and B) Curve 1 is for DsbC. Curves 2−4 are for DsbC in 0.1 M DTT, 3 M GdnHCl, and 3 M GdnHCl and 0.1 M DTT, respectively. Curve 5 is for G49R. Curve 6 is for G49R in 3 M GdnHCl. (C and D) Curves 1−3 are for DsbC, G49R, and Y52W, respectively.

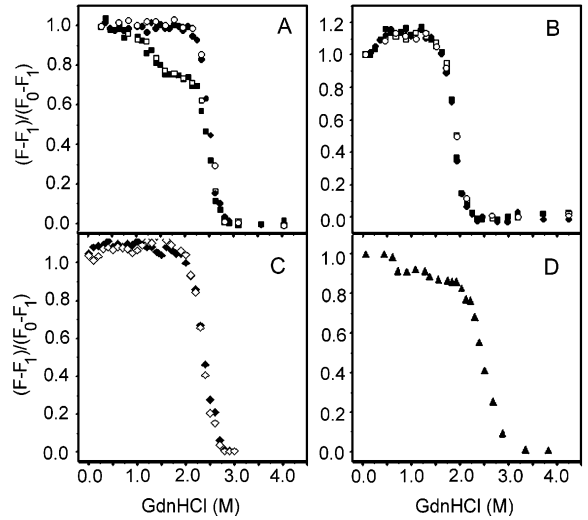

FIGURE 3: Equilibrium unfolding and refolding of DsbC proteins. Unfolding (■ and ●) of DsbC at 5 μM was performed by incubation with different concentrations of GdnHCl in the absence (A) and presence (B) of 0.1 M DTT at 25 °C for 20 h. Refolding (□ and ○) of 250 μM DsbC fully denatured in 4 M GdnHCl in the absence (A) and presence (B) of 0.1 M DTT was carried out by 50-fold dilution into a GdnHCl solution to make the final GdnHCl concentration as indicated and incubation at 25 °C for 2 h. The fluorescence intensities at 315 nm in the absence of DTT (A) and 320 nm in the presence of DTT (B) with excitation of 280 nm (■ and □) and at 320 (A) and 327 nm (B) with excitation at 295 nm (● and ○) were measured. (C) Unfolding of G49R under the same condition that was used for DsbC was assessed with excitation at 280 (◆) and 295 nm (◇). (D) Ellipticity at 222 nm of the CD spectrum of DsbC unfolded by GdnHCl in the absence of DTT. All the data were normalized as $(F - F_1)/(F_0 - F_1)$. F values were determined at the indicated GdnHCl concentration; F_0 and F_1 are the values of native and fully denatured (with 3.0 M GdnHCl) proteins, respectively.

Cys^{141}−Cys^{163}, in each subunit are reduced. As shown in Figure 2A, the maximum emission wavelength of intrinsic fluorescence spectra of DsbC excited at 280 nm red-shifted from 315 to 320 nm with no intensity change after reduction, and further to 350 nm with dramatically decreased intensity when denatured with 3.0 M GdnHCl either in the presence or in the absence of DTT. The fluorescence spectrum excited at 295 nm showed that the reduction with DTT increased the intensity and also shifted the maximal emission from 320 to 327 nm, which shifted further to 350 nm with markedly decreased intensity when denatured (Figure 2B). G49R exhibited fluorescence spectra similar to that of DsbC (Figure 2A,B). In contrast, Y52W exhibited greatly increased fluorescence intensity with the maximal emission at 335 nm excited at either 280 (Figure 2C) or 295 nm (Figure 2D), indicating that the fluorescence of Y52W is mainly contributed by Trp^{52}.

In contrast to the dimeric DsbC, G49R failed to assist the reactivation of denatured D-glyceraldehyde-3-phosphate dehydrogenase upon dilution and showed much lower isomerase and thiol-disulfide reductase activities. Y52W showed the same reductase, isomerase, and chaperone activities as DsbC. These results are summarized in Table 2.

Equilibrium Unfolding and Refolding. In the absence of DTT, the unfolding of DsbC determined by fluorescence excited at 295 nm exhibited a two-state transition curve with increasing GdnHCl concentrations from 0 to 4.0 M (Figure 3A). The fluorescence intensity showed no change until the GdnHCl concentration increased to 1.8 M and then dropped sharply with a midpoint at 2.3 M GdnHCl. In contrast, the unfolding measured with excitation at 280 nm exhibited a three-state transition curve with a pronounced plateau at GdnHCl concentrations of 1.4−1.8 M, indicating an intermediate state. The midpoints of the two transitions were at 1.1 and 2.3 M GdnHCl, respectively (Figure 3A). In the presence of 0.1 M DTT, the unfolding curves of DsbC excited either at 280 or 295 nm showed a three-state transition with a pronounced plateau for the intermediate state in a GdnHCl concentration range of 0.4−1.3 M. The midpoints of the two transitions are at 0.3 and 1.7 M GdnHCl, respectively (Figure 3B). Refolding curves of DsbC are the same as the unfolding curves excited either at 280 nm (Figure 3A) or at 295 nm (Figure 3B), indicating that the unfolding of DsbC over this GdnHCl concentration range is thermodynamically reversible. When excited at either 280 or 295 nm, monomeric G49R showed similar two-state transition unfolding curves with midpoints at 2.3 M (Figure 3C). The change in the ellipticity values at 222 nm of the CD spectra upon unfolding of DsbC also displayed a three-state transition curve with a plateau in the same range of GdnHCl concentrations (Figure 3D) as that observed in the fluorescence emission curve with excitation at 280 nm.

The concentration dependence of DsbC and Y52W unfolding is shown in Figure 4. The unfolding curve for dimeric DsbC at 1, 5, and 20 μM monitored by intrinsic fluorescence with excitation at 280 nm changed slightly in the first transition of 0−2.0 M GdnHCl but did not change at all in the second transition (Figure 4A). In contrast, the unfolding of Y52W at 0.5, 2, and 20 μM excited at 280 (Figure 4B) and 295 nm (Figure 4C) showed three-state transition profiles with the first transition markedly right-shifted with increasing protein concentrations in a range of 0−2.0 M GdnHCl but little shift in the second transition from 2.0 to 3.0 M GdnHCl.

Figure 5 shows phase diagrams representing the unfolding of DsbC proteins. The phase diagram for DsbC and Y52W

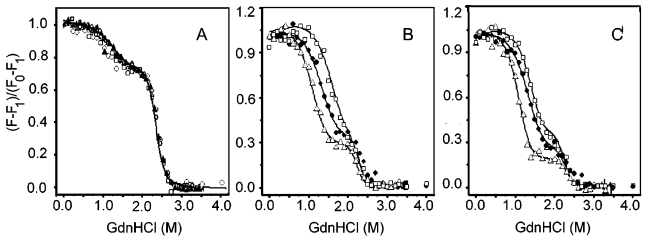

FIGURE 4: Protein concentration dependence of equilibrium unfolding of DsbC and Y52W. Unfolding of DsbC (A) at 1 (○), 5 (▲), and 20 μM (□) and of Y52W (B and C) at 0.5 (△), 2 (●), and 20 μM (□) was monitored by fluorescence intensity at 315 nm with excitation at 280 nm (A and B) and at 320 nm with excitation at 295 nm (C). Solid curves were calculated using the appropriate thermodynamic parameters given in Table 3 and further normalized. The curve of DsbC is calculated for 5 μM.

consists of two linear parts, corresponding to GdnHCl concentrations of 0−2.0 and 2.0−3.0 M, respectively (panels A and B of Figure 5, respectively). This indicates that the unfolding of these two proteins follows a three-state model with the formation of an intermediate in 0−2.0 M GdnHCl. The phase diagram for G49R (Figure 5C) is a straight line, consistent with the predicted behavior for a two-state model. The phase diagrams for excitation at 280 nm are the same as those for excitation at 295 nm (data not shown).

Native DsbC eluted from a size-exclusion column as a single peak with an apparent molecular mass of 58 kDa, indicating a dimer. The DsbC denatured at GdnHCl concentrations of <0.4 M without DTT appeared smaller than the native molecule and remained unchanged until 1.7 M (Figure 6A,B). A new peak at a smaller elution volume was apparent when the GdnHCl concentration was increased to 1.9 M. With increasing GdnHCl concentrations, the magnitude of the first peak decreased and disappeared at GdnHCl concentrations of >2.4 M, while the new peak appeared with an elution volume that decreased until 3 M GdnHCl. In the presence of DTT (Figure 6C,D), the second peak appeared at 1.6 M GdnHCl and increased in magnitude with a decreasing elution volume until 2.4 M GdnHCl while the first peak disappeared at 1.9 M.

Sedimentation velocity experiments were performed to identify the association state of DsbC as a function of GdnHCl concentration. These experiments (Figure 7) showed that the average molecular mass of native DsbC (48 kDa), corresponding to a dimer, decreased to 24 kDa with increasing GdnHCl concentrations over the range from 0 to 2.0 M. These experiments demonstrate that the first transition in the unfolding process is accompanied by the dissociation of the dimer to the monomer.

By using eq 4 (Table 1), which links the global fluorescence intensity and the concentrations of GdnHCl, the equilibrium folding profiles of DsbC excited at 280 nm and of Y52W excited at both 280 and 295 nm were fitted to a three-state model via a monomeric intermediate (Table 1, right column, eq 1), and the equilibrium folding curves of G49R excited at both 280 and 295 nm were fitted to a two-state model (Table 1, left column, eq 1). The unfolding reaction is characterized by four thermodynamic parameters (Table 3): the free energies for the dissociation of the native dimer and for the unfolding of the monomeric intermediate in the absence of GdnHCl ($\Delta G_{NI}^{H_2O}$ and $\Delta G_{IU}^{H_2O}$, respectively) and the coefficients of GdnHCl concentration dependence (m_{NI} and m_{IU}, respectively). The global average values of the thermodynamic parameters, ΔG^{H_2O} and m, calculated from the data at different protein concentrations by eqs 13 and 14 in Table 1, were as follows: 107 ± 4 kJ/mol and 40.0 ± 2.4 kJ mol^{-1} M^{-1} for DsbC, 78.6 ± 2.3 kJ/mol and 62.1 ± 2.7 kJ mol^{-1} M^{-1} for DsbC treated with DTT, and 107.9 ± 1.7 kJ/mol and 40.7 ± 0.6 kJ mol^{-1} M^{-1} for Y52W, respectively.

The population fractions of different conformational states of Y52W at three protein concentrations as functions of GdnHCl concentration, f_N, f_I, and f_U (Figure 8), were calculated from the thermodynamic parameters given in Table 3. Two characteristic concentrations of GdnHCl were deduced from these population fractions: $f_N^{-1}(0.5)$, at which half of the DsbC molecules were dissociated, and $f_U^{-1}(0.5)$, at which half of the monomers were unfolded (Table 3). These characteristic concentrations showed an effect of the total protein concentrations on the population fractions of the different conformational states, as expected for the unfolding of a dimeric protein (*21*). The values of $f_N^{-1}(0.5)$ for Y52W increased greatly and that for DsbC only slightly with increasing protein concentrations, while the values of $f_U^{-1}(0.5)$ for both Y52W and DsbC did not change.

Kinetics of Unfolding and Refolding. Figures 9 and 10 illustrate typical kinetic traces of unfolding and refolding of the DsbC proteins, respectively. Kinetic constants k_i obtained by fitting the kinetic curves in Figure 9 to eq 15 are listed in Table 4. Unfolding of DsbC (Figure 9A) and Y52W (Figure 9B) in 3 M GdnHCl displays multiphasic unfolding kinetics, and the residuals for fitting to a single and a double exponential show systematic variation, which were removed by fitting to a triple exponential. The data for unfolding of G49R (Figure 9C) fit well to a double-exponential equation, as do the data for unfolding of DsbC in the presence of 0.1 M DTT (Figure 9D), but to a single-exponential equation when DTT was present (Figure 9E). Refolding of DsbC proteins, either in the presence or in the absence of 0.1 M DTT, displays double-exponential kinetics (Figure 10). With two excitation wavelengths of 280 and 295 nm (data not shown), the kinetic parameters for unfolding and refolding do not exhibit any significant difference.

DISCUSSION

Intrinsic Fluorescence of DsbC. In each DsbC subunit, there are eight Tyr residues, among which only Tyr^{171} and subordinately Tyr^{38} and Tyr^{52} contribute to the bulk fluorescence of the molecule (*9*), and only one Trp at position 140 next to the non-active site disulfide bond, Cys^{141}−Cys^{163}, exposed partially to solvent (*5*). The fluorescence excited at 295 nm is primarily contributed by Trp^{140} and that excited at 280 nm by Tyr^{171}, Tyr^{38}, Tyr^{52}, and Trp^{140}. In Y52W, the fluorescence excited at 295 nm is primarily contributed by Trp^{52} and subordinately by Trp^{140}. Denaturation in GdnHCl unfolds the molecule, leading to great decrease in fluorescence intensity with emission markedly red-shifted.

Two Single-Site Mutants, G49R and Y52W. To specify the accurate mechanism of unfolding of dimeric DsbC, we compared folding profiles of dimeric DsbC and an engineered monomeric G49R. In the crystal structure of DsbC, Gly^{49} is located between two consecutive β-strands, 4 and 5, which are the core of the dimerization interface of the two subunits

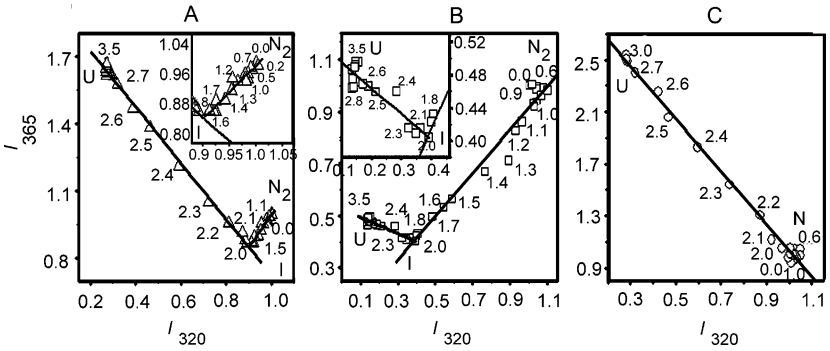

FIGURE 5: Phase diagrams representing the unfolding of DsbC proteins denatured in GdnHCl at different concentrations. DsbC (A), Y52W (B), and G49R (C) at 5 μM were denatured as described in the legend of Figure 3. The GdnHCl concentrations are indicated in the vicinity of the corresponding symbols. I_{320} and I_{365} are the fluorescence intensities at 320 and 365 nm, respectively, with excitation at 295 nm. N_2/N is the native state. I is the monomeric intermediate state. U is the unfolded state. The inset shows the details in the crossing part of the two lines.

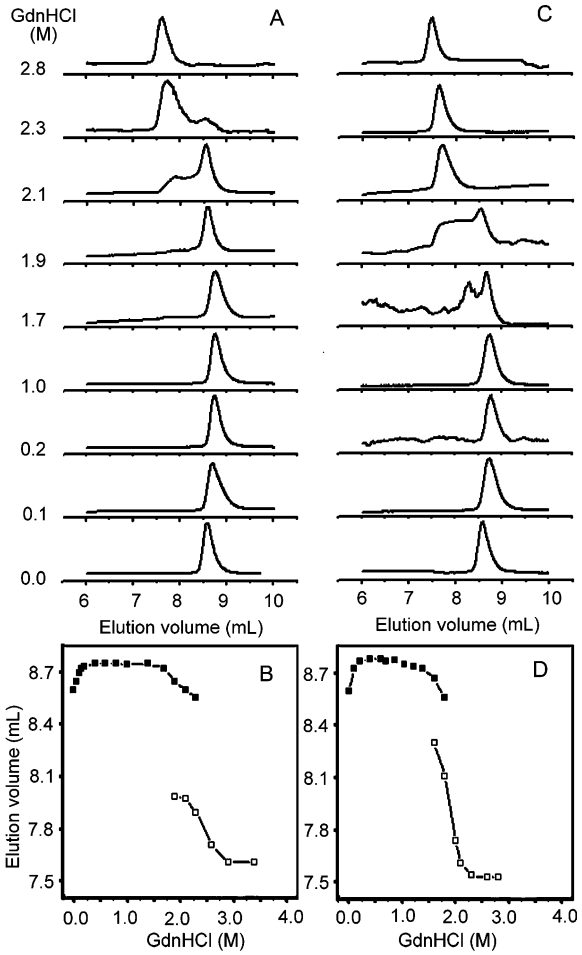

FIGURE 6: Size-exclusion chromatography profiles of DsbC denatured in GdnHCl at different concentrations. DsbC was denatured as described in the legend of Figure 3 in the absence (A and B) and presence (C and D) of 0.1 M DTT and then eluted using a SEC-250 column in the same concentrations of GdnHCl as indicated (A and C). (B and D) Elution volumes for the first (■) and second (□) elution peak in panels A and C, respectively.

(Figure 1). The substitution of the highly conserved small residue (Gly^{49}) with a large positively charged residue (Arg) impairs the association and prevents dimerization but appears not to cause a significant conformational change in the monomer with respect to the size-exclusion chromatography behavior (Table 2) (*6*), the CD spectrum (data not shown), and the intrinsic fluorescence spectrum (Figure 2). The

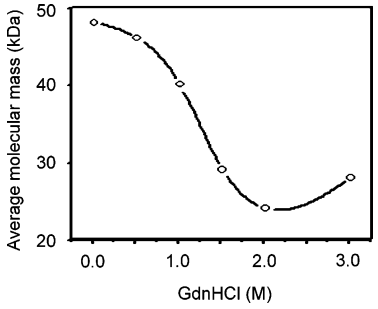

FIGURE 7: Average molecular mass of DsbC denatured in GdnHCl at different concentrations. DsbC was denatured as described in the legend of Figure 3. The average molecular mass of DsbC denatured in GdnHCl at different concentrations was determined by using sedimentation velocity as described in the text.

unfolding of the monomeric G49R can thus be taken as a folding model of the DsbC subunit with no dimeric intermediate. The results in this study show that the unfolding of G49R is a simple two-state process whether monitored by fluorescence with excitation at 280 or 295 nm. The lower fluorescence intensity of G49R might be caused by solvent quenching of the fluorescence of Tyr^{38} and Tyr^{52} in the N-terminal domain (*22*), as these two chromophores could be more exposed in the monomer than in the dimer. The unfolding of DsbC measured by intrinsic fluorescence with excitation at 280 nm exhibited a three-state transition curve, indicating an equilibrium unfolding intermediate.

The protein concentration dependence of unfolding profiles is usually taken to signify a dissociation step in folding transitions of dimeric proteins (*21*). No significant protein concentration dependence of the unfolding of DsbC was detected with excitation at 280 nm. To define the association state of the DsbC folding intermediate, we sought a dimeric mutant which could report spectral changes related to the dissociation of the two subunits during unfolding. We noticed first that Tyr^{52} in β5 (Figure 1) is located in the edge but not in the center of the dimerization interface and Tyr^{38} in β3 is located close to but not at the dimerization interface. Second, substitution of Tyr^{52} or Tyr^{38} with Trp would not interfere with the steric arrangement in this microenvironment. Third, substitution of Tyr^{52} or Tyr^{38} with Trp should produce stronger fluorescence excited at 295 nm. We prepared Y52W, which was shown to be a dimer by size-exclusion chromatography with a CD spectrum similar to that of DsbC (data not shown) and the same reductase,

Table 3: Thermodynamic Parameters Obtained from Equilibrium Unfolding of DsbC Proteins by GdnHCl

		Three-State Model ($N_2 \leftrightarrow 2I \leftrightarrow 2U$)					
	[protein] (μM)	$\Delta G_{NI}^{H_2O}$[a] (kJ/mol)	m_{NI}[a] (kJ mol^{-1} M^{-1})	$\Delta G_{IU}^{H_2O}$[a] (kJ/mol)	m_I[a] (kJ mol^{-1} M^{-1})	$f_N^{-1}(0.5)$[b] (M)	$f_U^{-1}(0.5)$[b] (M)
DsbC	1	49.9 ± 0.4	15.4 ± 0.2	55.3 ± 0.8	23.7 ± 0.2	1.02 ±0.002	2.33 ± 0.003
	5	49.8 ± 0.02	14.9 ± 0.8	56 ± 6	25 ± 2	1.3 ±0.0004	2.2 ± 0.2
	20	47.2 ± 4	14.8 ± 0.8	63 ± 6	27 ± 2	1.38 ± 0.09	2.3 ± 0.2
	mean	49 ± 2	15.0 ± 0.4	58 ± 5	25 ± 2		
reduced DsbC[c]	5	36.8 ± 2.3	38.0 ± 2.4	41.8 ± 0.3	24.1 ± 0.3	0.1 ± 0.01	1.7 ± 0.2
Y52W	0.5	52.6 ± 0.002	16.7 ± 0.2	54.6 ± 0.7	24.4 ± 0.2	0.99 ± 10^{-5}	2.24 ± 0.002
	1	51.8 ± 1	16.0 ± 0.08	55.6 ± 0.2	23.8 ± 0.1	$1.09 \pm 2 \times 10^{-3}$	$2.34 \pm 3 \times 10^{-4}$
	2	54.1 ± 1.5	17.0 ± 0.2	56.4 ± 0.6	24.0 ± 0.6	1.29 ± 0.01	2.35 ± 0.01
	5	52.8 ± 0.5	16.7 ± 0.8	54.9 ± 0.7	24.1 ± 0.1	1.35 ± 0.01	2.28 ± 0.001
	20	52.5 ± 0.02	17.0 ± 0.5	54.2 ± 1.4	23.8 ± 1.1	$1.51 \pm 2 \times 10^{-4}$	2.28 ± 0.03
	mean	52.8 ± 0.8	16.7 ± 0.4	55.1 ± 0.9	24.0 ± 0.2		

	Two-State Model ($N \leftrightarrow U$)			
	[protein] (μM)	$\Delta G_{NU}^{H_2O}$[a] (kJ/mol)	m_{NU}[a] (kJ mol^{-1} M^{-1})	$f_N^{-1}(0.5)$[b] (M)
G49R	5	45.8 ± 2.1	19.3 ± 0.9	2.37 ± 0.04

[a] Unfolding was monitored by fluorescence intensity as described in the legend of Figure 3. The thermodynamic parameters were obtained by fitting the experimental data to eqs 1−14 in Table 1. Each entry corresponds to the mean ± the standard deviation ($n = 3-5$). [b] $f_N^{-1}(0.5)$ and $f_U^{-1}(0.5)$ are the concentrations of GdnHCl where $f_N([GdnHCl]) = 0.5$ and $f_U([GdnHCl]) = 0.5$, respectively. Thermodynamic parameters were obtained by fitting the experimental data to eq 4 in Table 1. The values of f_N, f_I, and f_U and of their roots were calculated from the thermodynamic parameters using eqs 7−9 in Table 1. Each entry corresponds to the mean ± the standard deviation ($n = 3-5$). [c] Treated with 0.1 M DTT at 25 °C for 20 h.

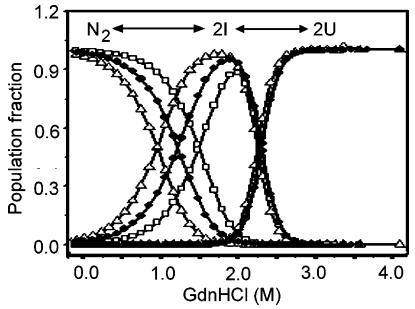

FIGURE 8: Fractions of the three conformational states of Y52W in equilibrium unfolding as a function of GdnHCl concentration. Y52W was denatured as described in the legend of Figure 3. The fractions f_N, f_I, and f_U of the native (N_2), intermediate (I), and unfolded (U) states of Y52W at 0.5 (△), 2 (●), and 20 μM (□) were calculated using thermodynamic parameters listed in Table 3 and eqs 7−9 in Table 1.

isomerase, and chaperone activities, indicating that this single mutation does not cause a significant conformational change. The mutant exhibited markedly increased fluorescence with excitation at either 280 or 295 nm (Figure 2C,D) and was thus used to examine the association state of the DsbC folding intermediate.

Equilibrium Folding of DsbC. The equilibrium curves of unfolding and refolding of DsbC, G49R, and Y52W over the GdnHCl concentration range measured by intrinsic fluorescence emission with excitation at 280 or 295 nm are in good superposition, indicating that the two processes are thermodynamically reversible. The unfolding of DsbC with increasing GdnHCl concentrations monitored by the changes in intrinsic fluorescence excited at 280 nm, ANS fluorescence excited at 370 nm (data not shown), and the CD spectrum all show a three-state transition, indicating the existence of at least one stable unfolding intermediate, which formed in the range of 0−2.0 M GdnHCl. In contrast, the fluorescence changes of DsbC in GdnHCl excited at 295 nm show a two-state transition, indicating no change in the intrinsic fluorescence contributed by only Trp^{140} in the folding intermediate. The partially unfolded intermediate formed at moderate GdnHCl concentrations showed more hydrophobic surface exposed as indicated by increased ANS fluorescence (data not shown).

Phase diagram analysis of fluorescence data of proteins is a sensitive method for the detection of any intermediate state (*13*) and was used to provide further characterization for three-state unfolding of DsbC and two-state unfolding of G49R. Although the unfolding of DsbC monitored at 320 nm with excitation at 295 nm showed a two-state transition profile, the diagram of I_{320} versus I_{365} showed two linear parts, indicating a three-state transition indeed.

The sedimentation velocity experiments with DsbC unfolded at different GdnHCl concentrations provide evidence that DsbC in 2 M GdnHCl exists as a monomer with an average molecular mass of 24 kDa (Figure 7). The unfolding of G49R, a monomeric molecule, showed a two-state transition curve excited at both 280 and 295 nm with the midpoint at 2.3 M GdnHCl, which is coincident with the midpoint of the second transition of DsbC unfolding monitored at 280 nm excitation, suggesting that the first transition (0−2.0 M GdnHCl) of DsbC unfolding is very likely involved in dissociation of the dimeric species and the second transition (2.0−3.0 M GdnHCl) represents the further unfolding of the monomeric species. Therefore, the stable folding intermediate of DsbC is monomeric. For a dimeric protein, the position of the unfolding−dissociation transition should depend on protein concentration (*21*). The unfolding of Y52W monitored by fluorescence showed a three-state transition curve, which was also confirmed by phrase diagram analysis, with an equilibrium plateau significantly lower than that of DsbC. The results suggest that the fluorescence of Trp^{52}, the main contributor to Y52W fluorescence, was partly quenched by solution after dissociation (*22*). The first transition of Y52W showed a strong protein concentration dependence, while the second transition

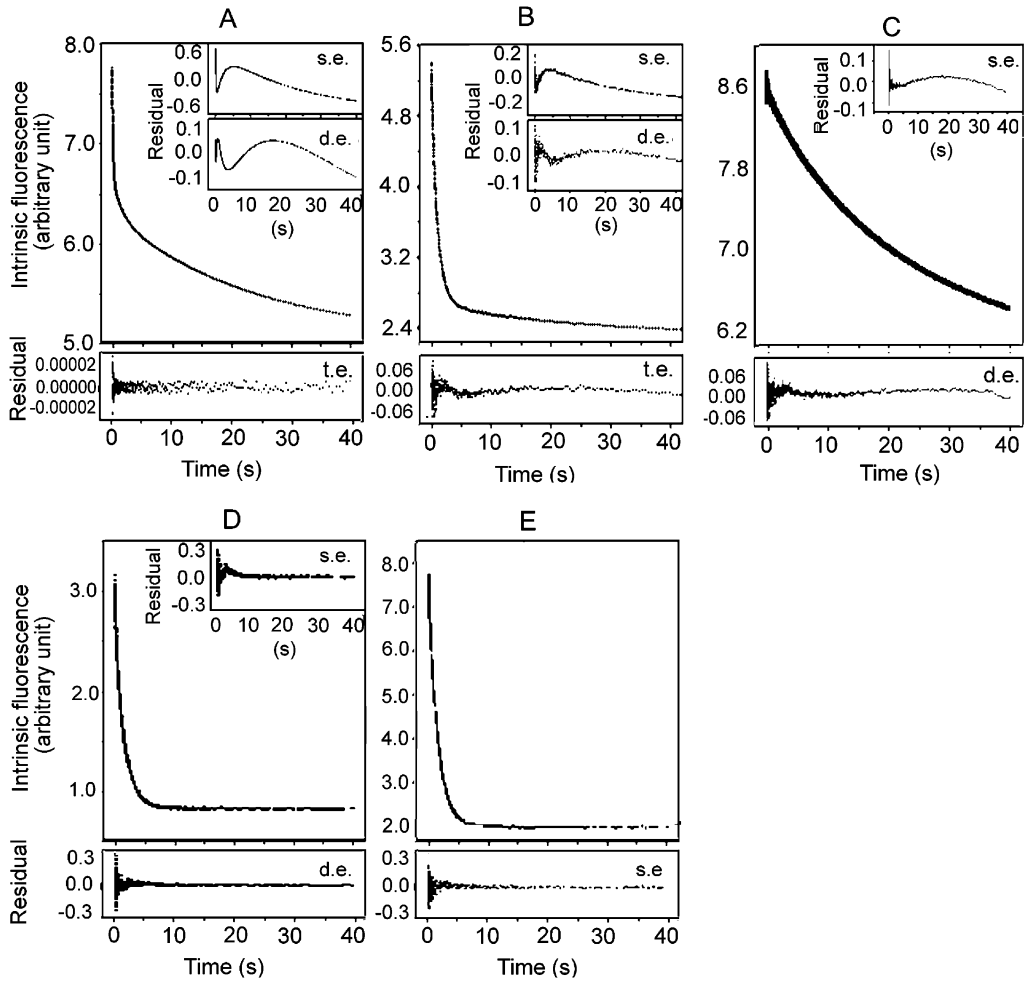

FIGURE 9: Kinetic traces for unfolding of DsbC proteins. Unfolding of DsbC (A and D), Y52W (B), and G49R (C and E) at 5 μM in 3.0 M GdnHCl without (A−C) and with (D and E) 0.1 M DTT was monitored at 315 nm with excitation at 280 nm. The quality of the fit to a single (s.e.), double (d.e.), or triple (t.e.) exponential is indicated by the residual (insets or below).

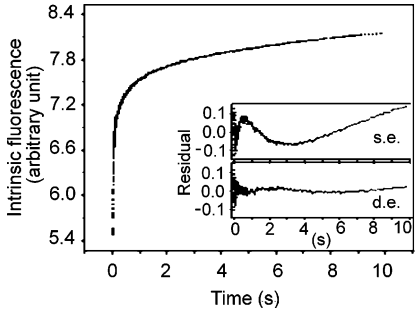

FIGURE 10: Kinetic trace for refolding of DsbC. The typical fitting kinetic trace for refolding of DsbC at 5 μM at a final concentration of GdnHCl of 0.27 M was monitored by the fluorescence intensity at 315 nm with excitation at 280 nm. The quality of the fit to a single (s.e.) and double (d.e.) exponential is indicated by the residual (insets).

showed no dependence. This result indicates that the fluorescence produced by Trp^{52} reports the changes caused by the dissociation of the dimer, providing direct evidence that dimeric DsbC unfolds through a monomeric intermediate. The second transition is caused by further unfolding of the monomer and does not exhibit a protein concentration dependence.

The first elution peak of DsbC denatured in different concentrations of GdnHCl on size-exclusion chromatography may indicate a mixture of native molecules and folding intermediates, the elution volume of which increased at low concentrations of GdnHCl until 1.0 M and then decreased with increasing GdnHCl concentrations. The second elution peak appearing in 1.9 M GdnHCl is attributed to the unfolded species.

In summarizing the above GdnHCl-induced equilibrium unfolding of wild-type DsbC and the two mutants measured using several methods, we propose a three-state transition folding model with a monomeric folding intermediate formed at mild GdnHCl concentrations of <2.0 M (Table 1). In transition 1, at GdnHCl concentrations of 0−2.0 M, the unfolding of the dimeric molecule, particularly unfolding of those structures responsible for association of the two subunits, results in dissociation of the homodimer. The monomeric folding intermediate is partially unfolded which is specified by the lower fluorescence intensity with maximum emission wavelength red-shifted, the higher ANS fluorescence specifying more exposed hydrophobic surface, the lower ellipticity at 222 nm of the CD spectrum, and the increased elution volume. This monomeric folding intermediate is stable in 1.0−2.0 M GdnHCl. In transition 2, the monomeric intermediate further unfolds with an increase in GdnHCl concentration. The unfolding of DsbC indicated that the hydrogen bonds between β-sheets responsible for the dimerization are very sensitive to GdnHCl and easily

Table 4: Kinetic Parameters of GdnHCl-Induced Unfolding and Refolding of DsbC Proteins[a]

	DsbC		G49R		Y52W		DsbC[b]		G49R[b]	
	280 nm	295 nm	280 nm	295 nm	280 nm	295 nm	280 nm	295 nm	280 nm	295 nm
unfolding										
k_1 (s^{-1})	6.8 ± 0.3	25.1 ± 0.3	0.60 ± 0.06	1.1 ± 0.1	46 ± 7	33 ± 5	10.4 ± 1.2	8.1 ± 1.4	0.664 ± 0.004	0.640 ± 0.004
k_2 (s^{-1})	0.63 ± 0.02	0.68 ± 0.05	0.047 ± 0.0007	0.057 ± 0.0007	1.060 ± 0.009	0.97 ± 0.002	0.658 ± 0.007	0.656 ± 0.007		
k_3 (s^{-1})	0.040 ± 0.001	0.047 ± 0.002			0.066 ± 0.006	0.056 ± 0.005				
refolding										
k_1 (s^{-1})	0.48 ± 0.02	0.52 ± 0.02	0.45 ± 0.006	0.51 ± 0.006	0.31 ± 0.008	0.15 ± 0.004	0.24 ± 0.02	0.35 ± 0.02		
k_2 (s^{-1})	0.027 ± 0.0002	0.029 ± 0.0002	0.030 ± 0.0002	0.040 ± 0.00007	0.027 ± 0.0002	0.017 ± 0.002	0.0234 ± 0.0009	0.026 ± 0.001		

[a] The unfolding and refolding of the DsbC proteins were carried out and monitored as described in the legends of Figures 9 and 10, respectively. The kinetic parameters were obtained by fitting the kinetic curves in Figures 9 and 10 to eq 15 with a P of <0.0001 and an R^2 of >0.99. Each entry corresponds to the mean ± the standard deviation. [b] In the presence of 0.1 M DTT.

impaired by low GdnHCl concentrations of 1.0−2.0 M before significant global conformational changes. When the GdnHCl concentration increases further, the structure of the monomeric intermediate collapses with a sharply decreased intrinsic fluorescence, ANS fluorescence, and ellipticity of CD, and the appearance of the second elution peak with a greatly decreased elution volume. At 3.0 M GdnHCl, the monomeric intermediate chain unfolded completely. To our knowledge, stable dimeric folding intermediates of DsbC have not been identified previously. A stable dimeric intermediate has been reported for the folding of EcHUα2 (*23*). EcHUα2 is a homodimer with a very compact structure stabilized by a pronounced hydrophobic core located underneath β-strands involving six Phe residues and by several aliphatic residues filling the gap between helix−turn−helix motifs. This dimeric structure is also stabilized by a hydrogen bond between the amine N-terminal atom of the Met^1 residue and the carbonyl O atom of the Ala^{14} residue of the other monomer. For the λ Cro repressor, which dimerizes through only one hydrophobic core formed by β-strands of two subunits, only a monomeric intermediate has been identified (*24*). The DsbC dimer is stabilized by hydrogen bonds, which are not sufficiently strong to maintain a stable dimeric folding intermediate.

The thermodynamic parameters of DsbC and Y52W (Table 3) at different protein concentrations remained constant (within experimental error) for a three-state model with a monomeric intermediate indicating that the unfolding curves of DsbC and Y52W are adequately described by this model (*20*). With increasing protein concentrations, $f_N^{-1}(0.5)$ moves to higher GdnHCl concentrations whereas $f_U^{-1}(0.5)$ does not, consistent with the population change of a monomeric intermediate (Figure 8).

Multiphasic Folding Kinetics of DsbC Proteins. Unfolding and refolding of DsbC, Y52W, and G49R assessed by fluorescence intensity showed multiphasic kinetics with excitation at both 280 and 295 nm. The unfolding curve of G49R (Figure 9) was fitted with two rate constants (designated k_1 and k_2 in Table 4); however, the values of these constants are close to those shown as k_2 and k_3 for DsbC and Y52W, respectively, indicating that G49R is devoid of the phase corresponding to k_1. The first phase with k_1 of DsbC and Y52W very likely corresponds to the dissociation of the dimer, termed the dissociation phase, and the phases with k_2 and k_3 could be termed unfolding phases. The unfolding monitored during 40−2000 s and the refolding during 500 s of dimeric and monomeric species showed little difference (data not shown). The presence of DTT makes the unfolding kinetics of DsbC switch from triple- to double-exponential with the third phase absent and that of G49R from double- to single-exponential with the second phase removed. These results indicated that the disruption of a non-active site disulfide bond by DTT has little effect on the dissociation phase of DsbC with the same k_1 but changes the unfolding kinetics from the monomeric intermediate to unfolded state through only one phase with the same k_2. Similarly, unfolding kinetics of G49R with non-active site disulfide bond reduced shows only one phase with the same k_1 of G49R in the absence of DTT (Table 4).

Biological Import of Dimerization. Monomerization of DsbC, by either removal of the association domain (*4*) or disruption of the dimerization interface by introduction of a

point mutation of G49 to R (*6*), eliminates chaperone activity as well as isomerase activity. Conversely, fusion of Trx, DsbA, and the *a* domain of protein disulfide isomerase, which are all monomeric with a Trx fold and low or no isomerase and chaperone activity, to the association domain of DsbC not only induces the hybrids to form a homodimer but also confers tremendously increased chaperone activity and isomerase activity. Thus, dimerization bestows new activities and allows DsbC to function as both a chaperone and an isomerase (*7*). It has been further suggested that DsbC evolved from Trx, and evolutionary pressure forced DsbC to find a mechanism, i.e., dimerization of the Trx domain, to allow its active site to be protected by DsbB-mediated oxidation so that the oxidative and reductive pathways can coexist in *Escherichia coli* periplasm (*6*). A few recent reports (*25*−*27*) support the idea that modular organization of proteins is a widely used thrifty and efficient strategy for protein evolution. In addition, we have noticed that compared with dimeric DsbC, the monomeric G49R is more sensitive to limited digestion by proteinase K and is less stable during purification and storage (data not shown). Therefore, dimerization gives more stability to the DsbC molecule and ensures the performance of the new functions of chaperone and isomerase.

The Non-Active Site Disulfide Bond Plays Important Roles in Stabilization of the DsbC Conformation. The two disulfide bonds in each subunit of DsbC are partially exposed to the solvent as shown in the crystal structure (*5*) and can be reduced by the reducing agent DTT even under nondenaturing conditions. Since the reduction of the active site disulfide does not alter the intrinsic fluorescence (*2*), the fluorescence changes caused by full reduction of the two disulfide bonds can be ascribed to the reduction of the unique non-active site disulfide bond, $Cys^{141}-Cys^{163}$. Although sulfur atoms of disulfide bonds are known as effective quenchers of Trp fluorescence, it has been shown recently that the two disulfide bonds do not directly quench the fluorescence of Trp^{140}. The side chains of the two neighboring residues, Cys^{141} and Trp^{140}, are oriented in opposite directions from the backbone, and the distance between the sulfur atoms of the disulfide bond and the indole ring of Trp^{140} is 8.6 and 8.9 Å, respectively (*9*). In addition, the sulfur atoms of Cys^{98} and Cys^{101} are 13.9 and 12.2 Å from the center of the indole ring, respectively. Therefore, the increase in the fluorescence intensity excited at 295 nm in the presence of DTT can only be ascribed to the conformation changes that resulted from the rupture of the $Cys^{141}-Cys^{163}$ disulfide, which could open up the structure of the molecule so that chromophores are more exposed to the environment with a red shift of the maximum emission wavelength. The reduction of the disulfides alleviates the difference between unfolding profiles of DsbC measured by fluorescence excitation at 295 (two-state transition) and 280 nm (three-state transition), resulting in the same three-state transition unfolding profile. This indicated that the break of the non-active site disulfide relieves its stabilization on the local conformation around Trp^{140} so that conformational change can occur in the folding intermediate. Moreover, reduction of the non-active site disulfide can cause further global conformational loosening, which resulted in the plateau for the equilibrium unfolding intermediate at lower concentrations of GdnHCl, 0.4−1.3 M, compared with 1.4−1.8 M for the unfolding in the absence of DTT, and the second transition also moved to lower GdnHCl concentrations with the midpoint decreased from 2.3 to 1.7 M. In addition, 3.0 M GdnHCl is required for the complete unfolding of DsbC, while 2.0 M GdnHCl is enough for the reduced species in DTT. Also, thermodynamic parameters $\Delta G_{NI}^{H_2O}$ and $\Delta G_{IU}^{H_2O}$ of DsbC in the presence of DTT are much lower than for DsbC in the absence of DTT. Disruption of the non-active site disulfide does not affect the dissociation phase of DsbC but results in the loss of the last unfolding phase. From what is presented here, we conclude that the non-active site disulfide bond plays an important role in stabilizing the conformation of the DsbC molecule. As in DsbA, the non-active site disulfide is located in a helical subdomain, which is inserted into the Trx fold. This might be a consequence of evolutionary selection for stability and capacity for new functions (*26*).

ACKNOWLEDGMENT

We thank Dr. Rudi Glockshuber for his generous gift of pDsbC and Dr. Sarah Perrett for advice on stopped-flow experiments. We are also grateful to Prof. C. L. Tsou for his continuous encouragement in this work. Helpful discussions with Prof. Zhixin Wang and Drs. Guoping Ren and Shengjian Li are appreciated.

REFERENCES

1. Nakamoto, H., and Bardwell, J. C. A. (2004) Catalysis of disulfide bond formation and isomerization in the *Escherichia coli* periplasm, *Biochim. Biophys. Acta 1694*, 111−119.
2. Zapun, A., Missiakas, D., Raina, E., and Creighton, T. E. (1995) Structural and functional characterization of DsbC, a protein involved in disulfide bond formation in *Escherichia coli*, *Biochemistry 34*, 5075−5089.
3. Chen, J., Song, J. L., Zhang, S., Wang, Y., Cui, D. F., and Wang, C. C. (1999) Chaperone activity of DsbC, *J. Biol. Chem. 274*, 19601−19605.
4. Sun, X. X., and Wang, C. C. (2000) The N-terminal sequence (residues 1-65) is essential for dimerization, activities, and peptide binding of *Escherichia coli* DsbC, *J. Biol. Chem. 275*, 22743−22749.
5. McMarthy, A. A., Haebel, P. W., Torronen, A., Rybin, V., Baker, E. N., and Metcalf, P. (2000) Crystal structure of the protein disulfide bond isomerase, DsbC, from *Escherichia coli*, *Nat. Struct. Biol. 7*, 196−199.
6. Bader, M. W., Hiniker, A., Regeimbal, J., Goldstone, D., Haebel, P. W., Riemer, J., Metcalf, P., and Bardwell, J. C. A. (2001) Turning a disulfide isomerase into an oxidase: DsbC mutants that imitate DsbA, *EMBO J. 20*, 1555−1562.
7. Zhao, Z., Peng, Y., Hao, S., Zeng, Z., and Wang, C. C. (2003) Dimerization by domain hybridization bestows chaperone and isomerase activities, *J. Biol. Chem. 278*, 43292−43298.
8. Liu, X. Q., and Wang, C. C. (2001) Disulfide-dependent folding and export of *Escherichia coli* DsbC, *J. Biol. Chem. 276*, 1146−1151.
9. Stepanenko, O. V., Kuznetsova, I. M., Turoverov, K. K., Huang, C. H., and Wang, C. C. (2004) Conformational change of the dimeric DsbC molecule induced by GdnHCl. A study by intrinsic fluorescence, *Biochemistry 43*, 5296−5303.
10. Bradford, M. M. (1976) A rapid and sensitive method for the quantitation of microgram quantities utilizing the principle of protein dye binding, *Anal. Biochem. 72*, 248−254.
11. Liang, S. J., Lin, Y. Z., Zhou, J. M., Tsou, C. L., Wu, P., and Zhou, Z. (1990) Dissociation and aggregation of D-glyceraldehyde-3-phosphate dehydrogenase during denaturation by guanidine hydrochloride, *Biochim. Biophys. Acta 1038*, 240−246.
12. Ellman, G. L. (1959) Tissue sulfhydryl groups, *Arch. Biochem. Biophys. 82*, 70−77.
13. Kuznetsova, I. M., Stepanenko, O. V., Turoverov, K. K., Zhu, L., Fan, Y. X., Zhou, J. M., Fink, A. L., and Uversky, V. N. (2002) Unraveling multistate unfolding of rabbit muscle creatine kinase, *Biochim. Biophys. Acta 1596*, 138−155.

14. Schuck, P. (2003) On the analysis of protein self-association by sedimentation velocity analytical ultracentrifugation, *Anal. Biochem. 320*, 104−124.
15. Kawahara, K., and Tanford, C. (1966) Viscosity and density of aqueous solutions of urea and guanidine hydrochloride, *J. Biol. Chem. 241*, 3228−3232.
16. Holmgren, A. (1979) Thioredoxin catalyzes the reduction of insulin disulfides by dithiothreitol and dihydrolipoamide, *J. Biol. Chem. 254*, 9627−9632.
17. Martínez-Galisteo, E., Padilla, C. A., Garcia-Alfonso, C., López-Barea, J., and Barcena, J. A. (1993) Purification and properties of bovine thioredoxin system, *Biochimie 75*, 803−809.
18. Lambert, N., and Freedman, R. B. (1983) Kinetics and specificity of homogeneous protein disulphide-isomerase in protein disulphide isomerization and in thiol-protein-disulphide oxidoreduction, *Biochem. J. 213*, 225−234.
19. Lyles, M. M., and Gilbert, H. F. (1991) Catalysis of the oxidative folding of ribonuclease A by protein disulfide isomerase: Dependence of the rate on the composition of the redox buffer, *Biochemistry 30*, 613−619.
20. Park, Y. C., and Bedouelle, H. (1998) Dimeric tyrosyl-tRNA synthetase from *Bacillus stearothermophilus* unfolds through a monomeric intermediate. A quantitative analysis under equilibrium conditions, *J. Biol. Chem. 273*, 18052−18059.
21. Neet, K. E., and Timm, D. E. (1994) Conformational stability of dimeric proteins: Quantitative studies by equilibrium denaturation, *Protein Sci. 3*, 2167−2174.
22. Szabo, A. G., and Rayner, D. M. (1980) Fluorescence decay of tryptophan conformers in aqueous solution, *J. Am. Chem. Soc. 102*, 554−563.
23. Ramstein, J., Hervouet, N., Coste, F., Zelwer, C., Oberto, J., and Castaing, B. (2003) Evidence of a thermal unfolding dimeric intermediate for the *Escherichia coli* histone-like HU proteins: Thermodynamics and structure, *J. Mol. Biol. 331*, 101−121.
24. Jana, R., Hazbun, T. R., Mollah, A. K., and Mossing, M. C. (1997) A folded monomeric intermediate in the formation of λ Cro dimer-DNA complexes, *J. Mol. Biol. 273*, 402−416.
25. Katzen, F., Deshmukh, M., Daldal, F., and Beckwith, J. (2002) Evolutionary domain fusion expanded the substrate specificity of the transmembrane electron transporter DsbD, *EMBO J. 21*, 3960−3969.
26. Martin, J. L. (1995) Thioredoxin: A fold for all reasons, *Structure 3*, 245−250.
27. Edeling, M. A., Guddat, L. W., Fabianek, R. A., Thöny-Meyer, L., and Martin, J. L. (2002) Structure of CcmG/DsbE at 1.14 Å resolution: High-fidelity reducing activity in an indiscriminately oxidizing environment, *Structure 10*, 973−979.
28. Grimsley, J. K., Scholtz, J. M., Pace, C. N., and Wild, J. R. (1997) Organophosphorus hydrolase is a remarkably stable enzyme that unfolds through a homodimeric intermediate, *Biochemistry 36*, 14366−14374.
29. Myers, J. K., Pace, C. N., and Scholtz, J. M. (1995) Denaturant m values and heat capacity changes: Relation to changes in accessible surface areas of protein unfolding, *Protein Sci. 4*, 2138−2148.
30. Pace, C. N. (1986) Determination and analysis of urea and guanidine hydrochloride denaturation curves, *Methods Enzymol. 131*, 266−280.

BI061511M